

Proceeding Paper

Microstructural and Mechanical Analysis of Aluminum Joints Under Varying Rotational Speeds in Friction Welding with Post-Quenching [†]

Bibit Sugito, Agus Dwi Anggono * , Agung Setyo Darmawan and Agus Hariyanto

Mechanical Engineering, Universitas Muhammadiyah Surakarta, Jl. Ahmad Yani, Pabelan 57162, Jawa Tengah, Indonesia; bibit.sugito@ums.ac.id (B.S.); asd145@ums.ac.id (A.S.D.); agus.hariyanto@ums.ac.id (A.H.)

* Correspondence: ada126@ums.id

[†] Presented at the 8th Mechanical Engineering, Science and Technology International Conference, Padang Besar, Perlis, Malaysia, 11–12 December 2024.

Abstract: This study examines the effects of rotational speed and post-weld quenching on aluminum friction-welded joints' microstructure, hardness, and mechanical properties. Tests were conducted at rotational speeds of 1250 rpm, 1350 rpm, and 1450 rpm, with elemental composition assessed via SEM-EDS, and the hardness and mechanical properties were measured. The results showed that aluminum (Al) was the primary element in all samples. Hardness increased with rotational speed, reaching 70 VHN at 1250 rpm, 80 VHN at 1350 rpm, and 81 VHN at 1450 rpm. The highest stress was recorded at 1350 rpm, with the lowest at 1450 rpm. The aluminum joints exhibited high stress and strain values, confirming their ductile nature. These findings highlight the significant influence of rotational speed and quenching on friction-welded aluminum's microstructural and mechanical behavior, providing insights for optimizing welding parameters for improved material performance in industrial applications.

Keywords: friction welding; rotational speed; aluminum joints; microstructure analysis; mechanical properties optimization



Academic Editors: Noor Hanita
Abdul Majid, Waluyo Adi Siswanto,
Tri Widodo Besar Riyadi,
Mohammad Sukri Mustapa, Nur
Rahmawati Syamsiyah and
Afif Faishal

Published: 29 January 2025

Citation: Sugito, B.; Anggono, A.D.;
Darmawan, A.S.; Hariyanto, A.
Microstructural and Mechanical
Analysis of Aluminum Joints Under
Varying Rotational Speeds in Friction
Welding with Post-Quenching. *Eng.
Proc.* **2025**, *84*, 20. [https://doi.org/
10.3390/engproc2025084020](https://doi.org/10.3390/engproc2025084020)

Copyright: © 2025 by the authors.
Licensee MDPI, Basel, Switzerland.
This article is an open access article
distributed under the terms and
conditions of the Creative Commons
Attribution (CC BY) license
([https://creativecommons.org/
licenses/by/4.0/](https://creativecommons.org/licenses/by/4.0/)).

1. Introduction

Friction welding is an increasingly adopted solid-state joining technique, which is precious for aluminum alloys used in aerospace and automotive industries. The method minimizes the issues associated with fusion welding, such as porosity and cracking, which are common in aluminum due to its high thermal conductivity and oxide layer formation [1]. Friction welding relies on rotational speed, friction time, and axial force, which are critical to achieving solid joints with minimal defects [2]. Studies highlight the unique challenges of welding aluminum, including controlling interfacial heat to avoid thermal degradation while ensuring sufficient bonding [3,4].

Rotational speed is a critical factor in friction welding that directly influences heat generation and material flow. Higher rotational speeds increase the heat at the interface, promoting plastic deformation and grain refinement through dynamic recrystallization. At optimal speeds, aluminum alloys achieve finer grains and improved mechanical properties [5,6]. However, excessive speed can lead to grain coarsening due to overheating, weakening the joint [7]. Research suggests that rotational speeds between 1200 and 1500 rpm effectively balance strength and ductility in aluminum joints [8,9].

Quenching is commonly applied as a post-weld heat treatment to refine the microstructure and enhance mechanical properties. In friction-welded aluminum, quenching

accelerates cooling, limiting grain growth and increasing hardness. Studies indicate that quenching after friction welding results in finer grains and increased tensile strength, although it may slightly reduce ductility [10,11]. Comparative studies of quenching with other heat treatments, like annealing and aging, show that quenching provides the best combination of hardness and strength, essential for load-bearing applications [12,13].

Advanced microstructural analysis techniques, particularly SEM (Scanning Electron Microscopy) and EDS (Energy Dispersive Spectroscopy), are pivotal in examining friction-welded aluminum joints. SEM provides detailed images of grain boundaries and phase distributions, while EDS allows elemental analysis across the weld line [14,15]. SEM–EDS analysis helps identify the presence of oxides or impurities, which may weaken weld integrity. Studies utilizing SEM–EDS confirm that increased rotational speed and post-weld quenching result in more homogeneous aluminum distribution and reduced impurity segregation [16,17].

The mechanical properties of aluminum friction welds, including hardness, tensile strength, and ductility, depend highly on rotational speed and post-weld treatments. Increased rotational speeds improve hardness and tensile strength due to finer grains and enhanced bonding. However, extremely high speeds can lead to brittle behavior. Studies report that friction welds quenched after welding exhibit increased hardness and strength but may experience reduced elongation [7,18]. Stress–strain analysis reveals that quenching achieves optimal mechanical performance at moderate rotational speeds, providing an ideal balance of strength and flexibility [19,20].

The microstructural changes induced by friction welding parameters directly correlate with mechanical performance. According to the Hall–Petch relationship, finer grains increase hardness and strength, as seen in quenched, high-speed friction welds of aluminum [21]. Elemental distribution and phase transformations further influence weld integrity, with well-distributed aluminum phases enhancing load-bearing capacity and resistance to crack initiation [22,23]. The optimization of welding parameters is essential for achieving a strong and ductile weld capable of withstanding mechanical stress without premature failure [24,25].

Despite advancements in understanding friction welding of aluminum, gaps remain in quantitative studies that correlate specific rotational speeds and quenching conditions with stress–strain behaviors. Future research should focus on real-time monitoring of microstructural changes during welding and post-treatment to fine-tune parameter selection [26,27]. Additionally, long-term performance tests, including fatigue and corrosion resistance, are recommended to establish more comprehensive guidelines for industrial applications of friction-welded aluminum [28,29].

The literature highlights that friction welding parameters, particularly rotational speed, and post-weld quenching, significantly influence aluminum joints' microstructural and mechanical properties. Optimal settings enhance hardness, tensile strength, and ductility, making aluminum welds suitable for demanding industrial applications. Further research in parameter optimization and testing under varying service conditions will expand the utility of friction-welded aluminum components.

2. Materials and Methods

2.1. Materials

The material used in this study is aluminum alloy A6061, as shown in Figure 1. It was chosen for its excellent weldability, good corrosion resistance, and high strength-to-weight ratio, making it ideal for industrial applications. The A6061 material was provided as solid cylindrical rods with a length of 100 mm and a diameter of 16 mm. These rods were

subsequently machined into test specimens, with specific shaping for tensile testing and surface preparation for hardness testing and microstructural analysis.



Figure 1. The A6061 material for friction welding.

2.2. Equipment and Experimental Setup

A range of specialized equipment was used for friction welding, machining, heat treatment, and testing. Detailed specifications for each piece of equipment are as follows:

- Friction welding machine: The friction welding process was conducted using a custom-built friction welding machine in the Mechanical Engineering Laboratory. The machine was equipped with a precision control system, enabling accurate adjustments to rotational speed, friction time, and axial force, which are critical to achieving consistent welding results. Rotational speeds were set at 1250 rpm, 1350 rpm, and 1450 rpm for this study.
- Lathe machine: A high-precision lathe (Brand: Haas ST-10, Haas Automation, Inc., California, USA.) was used to prepare the specimens for tensile testing by machining the cylindrical aluminum rods into a bone shape with threads at each end. This threading ensures secure gripping during the tensile test, preventing slippage. The Haas ST-10 provides machining precision within ± 0.02 mm, maintaining uniformity across all specimens.
- Tensile testing machine: Tensile tests were conducted using an Instron 5982 Universal Testing Machine, capable of handling loads up to 100 kN. This machine, equipped with Bluehill Universal software, records tensile strength, yield strength, and strain data. The machine's precision load cell ensures high accuracy in measurement, and testing was conducted at a constant crosshead speed of 1 mm/min to maintain consistency across specimens.
- Furnace machine: Heat treatment was carried out in a high-temperature laboratory furnace (Brand: Nabertherm LHT 02/17 LB, Nabertherm GmbH, headquartered in Lilienthal, Germany) capable of reaching temperatures up to 1650 °C. The specimens underwent a quenching process immediately after heat treatment. The furnace's digital control system allowed for precise temperature setting and uniform heating, essential for maintaining consistency across samples.
- Hardness testing machine: Vickers hardness tests were performed using a Mitutoyo HM-210 hardness tester. The machine was set to a load of 500 g with a dwell time of 10 s. This tester provides a high degree of accuracy in hardness measurements within the 5–1500 VHN range. Hardness values were taken at multiple points across the weld interface to assess hardness distribution and identify any changes due to friction welding and post-weld heat treatment.
- Scanning Electron Microscope (SEM) and Energy Dispersive Spectroscopy (EDS): Microstructural and elemental analyses were performed using a JEOL JSM-IT500 SEM (JEOL Ltd., Tokyo, Japan). with integrated EDS capabilities. The SEM offers a resolution of 3 nm at 30 kV, which allows for detailed imaging of grain structures and weld interfaces. EDS was used to analyze the elemental composition across the weld

zone to confirm the presence and distribution of aluminum and any alloying elements or impurities. SEM–EDS data provided insights into the changes in microstructure and phase distribution induced by different welding parameters and heat treatments.

2.3. Specimen Preparation

Cutting and machining: Aluminum A6061 rods were first cut to 100 mm using a band saw. The specimens were then machined on the Haas ST-10 lathe to achieve the specified diameter of 16 mm. Bone-shaped tensile test specimens were created according to ASTM E8 standards, with threads machined at both ends to facilitate secure gripping during tensile testing.

Before welding, each specimen was polished using silicon carbide abrasive papers (grit sequence: 400, 800, and 1200) to remove any oxide layer and surface contaminants. This step ensured consistent contact during welding and reduced the potential for surface imperfections affecting the results.

2.4. Friction Welding Process

The friction welding process was conducted on the laboratory friction welding machine, with rotational speeds set at 1250 rpm, 1350 rpm, and 1450 rpm. The following parameters were carefully controlled and recorded for each welding trial:

- Rotational speed: set at each of the three predetermined speeds to assess the effect of rotational speed on weld quality.
- Friction time: each specimen was subjected to a standardized friction time to ensure uniform exposure to frictional heat.
- Axial force: a constant axial force of 10 kN was applied throughout the welding process to maintain pressure at the weld interface.

2.5. Heat Treatment (Quenching)

The specimens underwent heat treatment in the Nabertherm LHT 02/17 LB furnace after the friction welding process. Each specimen was heated to a target temperature and then rapidly cooled through quenching in water. This process was intended to refine the microstructure, increase hardness, and improve the mechanical properties of the welded joints. The controlled quenching process minimized residual stresses and helped achieve uniform hardness across the weld zone.

2.6. Testing and Analysis

Tensile testing: After heat treatment, tensile tests were conducted on the Instron 5982 Universal Testing Machine (Instron, Massachusetts, USA) to assess each specimen's strength, yield point, and ductility. The data obtained from these tests provided insights into the effects of welding parameters and heat treatment on the mechanical properties of the aluminum joints.

Hardness testing: Vickers hardness measurements were taken across the weld interface to evaluate the hardness profile and identify changes due to friction welding and quenching. Multiple measurements were made from the center of the weld outward to capture the hardness gradient across the weld zone.

Microstructural and elemental analysis: SEM–EDS was used to examine the microstructure and elemental distribution at the weld interface. The JEOL JSM-IT500 SEM provided high-resolution images of the grain structure, while EDS analysis identified the distribution of elements such as aluminum, magnesium, and any impurities. These analyses were crucial for understanding the effects of welding parameters and heat treatment on the welded joints' microstructural evolution and alloy composition.

3. Results and Discussion

3.1. Friction Welding and Rotational Speed Effects

This study conducted friction welding at rotational speeds of 1250, 1350, and 1450 rpm with a friction time of 7 s. Rotational speed is a crucial parameter in friction welding, as it directly impacts the heat generated and the material flow at the weld interface. With increasing rotational speed, the generated heat increases, enhancing plastic deformation and bond formation. At 1250 rpm, the welding interface was exposed to moderate heat, resulting in a stable yet less refined structure than at higher speeds. The specimen welded at 1350 rpm exhibited optimal properties due to sufficient heat for dynamic recrystallization without excessive grain coarsening. At 1450 rpm, although there was significant heat generation, slight over-softening of the material occurred, which reduced the tensile strength and made the weldless ductile. This demonstrates that while higher speeds enhance bonding, an optimal range must be maintained to prevent overheating and reduce potential weaknesses in the joint.

3.2. Heat Treatment and Quenching

After friction welding, each specimen underwent heat treatment, including quenching from 550 °C for 45 min. Quenching is essential for grain refinement and enhancing the hardness and tensile properties by rapidly cooling the material and solidifying the microstructure. The rapid cooling suppresses the formation of coarser grains, ensuring a refined and uniform grain structure in the aluminum alloy. The microstructure of the quenched specimens revealed smaller grains and increased hardness due to minimized grain growth, which is typical of quenched A6061 aluminum. This heat treatment also improved the material's ductility, as the uniform grain size contributes to enhanced toughness without compromising strength. The quenching process thus effectively balanced the aluminum's microstructure, reinforcing the weld area and improving its mechanical performance.

3.3. Tensile Testing Results

The tensile tests were conducted to evaluate the strength and ductility of the weld joints at each rotational speed, as described in Figure 2. The tensile strength varied significantly with rotational speed, peaking at 1350 rpm. At 1250 rpm, the tensile strength was lower due to insufficient plastic deformation at the weld interface, leading to a less cohesive joint. The 1350 rpm specimen, with the highest tensile strength, benefitted from adequate heat and plastic flow that optimized interfacial bonding. This optimal tensile strength was recorded at 242.72 MPa, with a notable strain of 33.44%, indicating good ductility. At 1450 rpm, the tensile strength declined slightly to 217.2 MPa due to the softening effect of excessive heat, which can compromise the bond's structural integrity. The results imply that an intermediate speed provides the most favorable balance between strength and ductility for aluminum joints in friction welding.

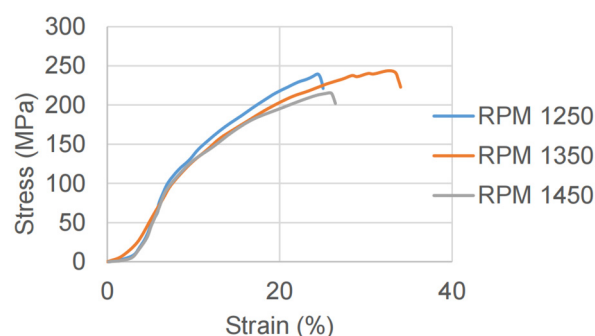


Figure 2. The influence of rotation to the stress–strain.

The fracture surfaces of the tensile test specimens were analyzed, showing typical ductile failure patterns with dimples and microvoids, confirming that the welded joints retained their ductility. The variation in stress–strain behavior across the three speeds highlights the importance of optimizing rotational speed to achieve desired mechanical properties in aluminum friction welding.

3.4. Hardness Testing Results

Figure 3 shows the microhardness results in all specimens' weld regions. Hardness testing revealed significant differences across the three welding speeds. At 1250 rpm, the hardness value was recorded at 70 VHN, which is comparatively low due to the reduced heat and plastic deformation. At 1350 rpm, hardness increased to 80 VHN, reflecting the refined grain structure and enhanced bond strength due to optimal heating conditions. For the 1450 rpm specimen, hardness was slightly higher at 81 VHN, suggesting additional hardening due to increased heat; however, this came with the trade-off of decreased tensile strength. The hardness profile indicated that quenching after welding contributed to a uniform hardness distribution across the weld area, ensuring a robust joint with minimized weaknesses.

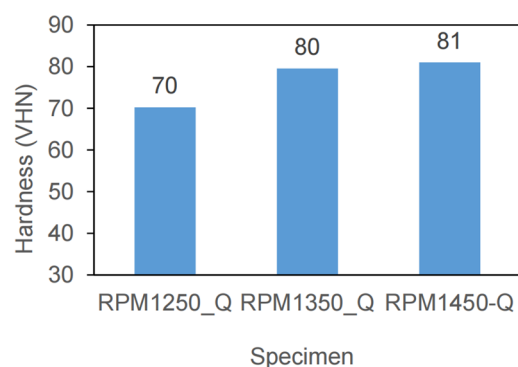


Figure 3. The results of microhardness of all specimens.

The observed increase in hardness with rotational speed aligns with the microstructural refinement noted in the SEM images, with finer grains providing resistance to indentation. This refinement and quenching suggest that heat treatment is essential for maintaining hardness in aluminum welds, especially at higher rotational speeds.

3.5. SEM and Microstructural Analysis

SEM imaging provided insights into the grain structure and phase distribution within the weld zone, as seen in Figure 4. At 1250 rpm (see Figure 4a), the SEM images displayed more oversized and irregular grains due to lower heat input, resulting in a less refined structure. At 1350 rpm (see Figure 4b), the microstructure was characterized by refined, equiaxed grains indicative of dynamic recrystallization at optimal heat levels. This grain refinement enhances strength and hardness, aligning with the observed tensile and hardness data. SEM revealed an ultra-fine grain structure at 1450 rpm (Figure 4c), but slight over-softening due to excess heat may have compromised the joint's toughness.

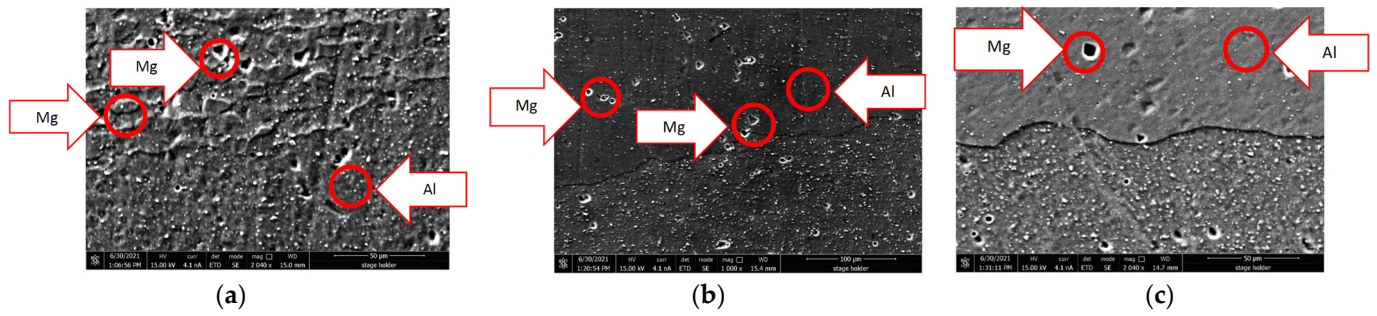


Figure 4. The SEM images of the weld region from friction welding conducted at varying rotational speeds: (a) 1250 rpm; (b) 1350 rpm; and (c) 1450 rpm.

The microstructural evolution observed at each speed underscores the importance of achieving controlled thermal cycles. The ideal microstructure, noted at 1350 rpm, demonstrated a balance of refined grains and stable phases, essential for maximizing hardness and ductility.

3.6. EDS Analysis and Elemental Composition

EDS analysis confirmed the elemental composition in the weld area, with aluminum as the primary element, supported by traces of magnesium and silicon, as illustrated in Figure 5. At 1250 rpm (Figure 5a), the aluminum content was 96.03%, with minor oxygen and carbon, possibly from surface contamination or oxidation. The EDS results at 1350 rpm (see Figure 5b) showed a slight reduction in aluminum concentration (95.67%) but increased distribution uniformity, suggesting enhanced diffusion of alloying elements. At 1450 rpm (Figure 5c), aluminum concentration was similar (96.78%), but a slight increase in oxygen indicated some surface oxidation due to prolonged exposure to high temperatures.

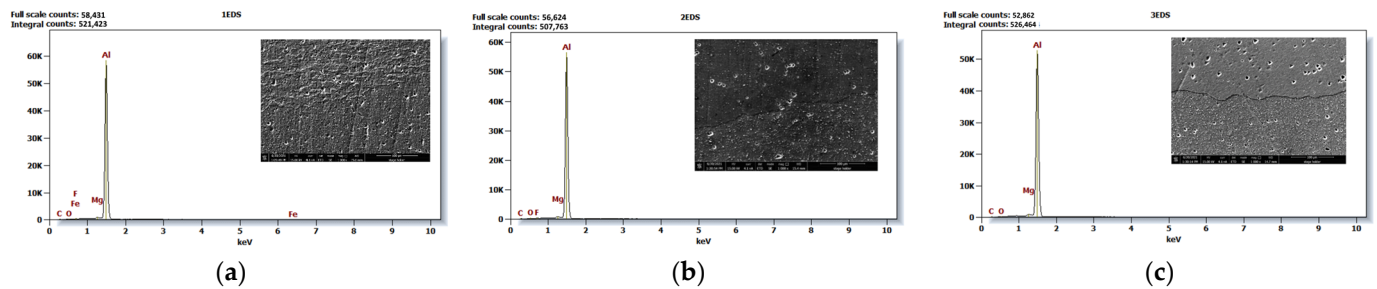


Figure 5. The EDS analysis results of the weld region from friction welding performed at different rotational speeds: (a) 1250 rpm; (b) 1350 rpm; and (c) 1450 rpm.

The magnesium content remained stable across all speeds, supporting the alloy’s stability and microstructural integrity during welding. The presence of magnesium contributes to the hardness and strength of the alloy, complementing the grain refinement observed in SEM analysis. The EDS results underscore the importance of controlling oxidation, especially at higher speeds, to maintain the quality of the weld interface.

4. Conclusions

The results of this study demonstrate that both rotational speed and post-weld quenching significantly impact the microstructure and mechanical properties of friction-welded aluminum A6061 joints. An intermediate rotational speed (1350 rpm) was identified as optimal, balancing tensile strength, hardness, and ductility due to sufficient heat input for grain refinement without excessive softening. Post-weld quenching effectively refined the

grain structure, enhancing hardness across the weld interface. SEM and EDS analyses corroborated these findings, revealing a refined, stable microstructure with limited oxidation.

These results suggest that by optimizing rotational speed and employing appropriate heat treatment, friction welding can produce high-quality aluminum joints with superior mechanical properties, suitable for industrial applications with critical strength and ductility.

Author Contributions: The author's contributions are as follows: the materials and equipment were produced by B.S., A.D.A. analyzed data, A.S.D. wrote the text, and the experimental procedures were conducted by A.H. All authors have read and agreed to the published version of the manuscript.

Funding: The Innovation and Research Office of Universitas Muhammadiyah Surakarta funded this study under the Tridharma Integration Research Scheme, contract number 071/A.3-III/FT/III/2021. The authors would also like to thank the Material Laboratory and Mechanical Engineering Department of Universitas Muhammadiyah Surakarta for their essential contributions to this project.

Institutional Review Board Statement: Not applicable.

Informed Consent Statement: Not applicable.

Data Availability Statement: No new data were created.

Acknowledgments: The authors would especially like to thank the Innovation and Research Office of Universitas Muhammadiyah Surakarta for their significant financial support. Additionally, we sincerely thank the Material Laboratory and Mechanical Engineering Department of Universitas Muhammadiyah Surakarta for their essential contributions that greatly enhanced our research.

Conflicts of Interest: The authors declare no conflicts of interest.

References

- Ahmed, M.M.Z.; Seleman, M.M.E.-S.; Fydrych, D.; Çam, G. Friction Stir Welding of Aluminum in the Aerospace Industry: The Current Progress and State-of-the-Art Review. *Materials* **2023**, *16*, 2971. [[CrossRef](#)] [[PubMed](#)]
- Çam, G.; Javaheri, V.; Heidarzadeh, A. Advances in FSW and FSSW of dissimilar Al-alloy plates. *J. Adhes. Sci. Technol.* **2022**, *37*, 162–194. [[CrossRef](#)]
- Elsheikh, A.H. Applications of machine learning in friction stir welding: Prediction of joint properties, real-time control and tool failure diagnosis. *Eng. Appl. Artif. Intell.* **2023**, *121*, 105961. [[CrossRef](#)]
- Mirzadeh, H. Grain refinement of magnesium alloys by dynamic recrystallization (DRX): A review. *J. Mater. Res. Technol.* **2023**, *25*, 7050–7077. [[CrossRef](#)]
- Guo, Z.; Ma, T.; Yang, X.; Tao, J.; Li, J.; Li, W.; Vairis, A. In-situ investigation on dislocation slip concentrated fracture mechanism of linear friction welded dissimilar Ti17($\alpha+\beta$)/Ti17(β) titanium alloy joint. *Mater. Sci. Eng. A* **2023**, *872*, 144991. [[CrossRef](#)]
- Yang, J.; Oliveira, J.; Li, Y.; Tan, C.; Gao, C.; Zhao, Y.; Yu, Z. Laser techniques for dissimilar joining of aluminum alloys to steels: A critical review. *J. Mech. Work. Technol.* **2022**, *301*, 117443. [[CrossRef](#)]
- He, C.; Wei, J.; Li, Y.; Zhang, Z.; Tian, N.; Qin, G.; Zuo, L. Improvement of microstructure and fatigue performance of wire-arc additive manufactured 4043 aluminum alloy assisted by interlayer friction stir processing. *J. Mater. Sci. Technol.* **2023**, *133*, 183–194. [[CrossRef](#)]
- Ma, Y.; Chen, H.; Zhang, M.-X.; Addad, A.; Kong, Y.; Lezaack, M.B.; Gan, W.; Chen, Z.; Ji, G. Break through the strength-ductility trade-off dilemma in aluminum matrix composites via precipitation-assisted interface tailoring. *Acta Mater.* **2023**, *242*, 118470. [[CrossRef](#)]
- Heidarzadeh, A.; Mironov, S.; Kaibyshev, R.; Çam, G.; Simar, A.; Gerlich, A.; Khodabakhshi, F.; Mostafaei, A.; Field, D.; Robson, J.; et al. Friction stir welding/processing of metals and alloys: A comprehensive review on microstructural evolution. *Prog. Mater. Sci.* **2021**, *117*, 100752. [[CrossRef](#)]
- Riyadi, T.W.B.; Sarjito; Anggono, A.D.; Masyrukan; Eryawan, A. Effect of Ni underlayer thickness on the hardness and specific wear rate of Cu in the laminated Ni/Cu coatings produced by electroplating. *AIP Conf. Proc.* **2018**, *1977*, 030050. [[CrossRef](#)]
- Zhai, M.; Wu, C.; Su, H. Influence of tool tilt angle on heat transfer and material flow in friction stir welding. *J. Manuf. Process.* **2020**, *59*, 98–112. [[CrossRef](#)]
- Li, J.; Li, Y.; Wang, F.; Meng, X.; Wan, L.; Dong, Z.; Huang, Y. Friction stir processing of high-entropy alloy reinforced aluminum matrix composites for mechanical properties enhancement. *Mater. Sci. Eng. A* **2020**, *792*, 139755. [[CrossRef](#)]

13. Dialami, N.; Cervera, M.; Chiumenti, M. Defect formation and material flow in Friction Stir Welding. *Eur. J. Mech.-A/Solids* **2020**, *80*, 103912. [[CrossRef](#)]
14. Boopathi, S. Experimental investigation and multi-objective optimization of cryogenic Friction-stir-welding of AA2014 and AZ31B alloys using MOORA technique. *Mater. Today Commun.* **2022**, *33*, 104937. [[CrossRef](#)]
15. Darmawan, A.S.; Anggono, A.D.; Yulianto, A.; Febriantoko, B.W.; Masyrukan, M.; Ginta, T.L.; Hamid, A. Effect of Shielded Metal Arc Welding on Microstructure, Hardness, and Tensile Strength of Nodular Cast Iron. *Adv. Sci. Technol.* **2024**, *141*, 21–26. [[CrossRef](#)]
16. Zhu, Z.; Hu, Z.; Seet, H.L.; Liu, T.; Liao, W.; Ramamurty, U.; Nai, S.M.L. Recent progress on the additive manufacturing of aluminum alloys and aluminum matrix composites: Microstructure, properties, and applications. *Int. J. Mach. Tools Manuf.* **2023**, *190*, 104047. [[CrossRef](#)]
17. Zeng, X.; Xue, P.; Wu, L.; Ni, D.; Xiao, B.; Wang, K.; Ma, Z. Microstructural evolution of aluminum alloy during friction stir welding under different tool rotation rates and cooling conditions. *J. Mater. Sci. Technol.* **2019**, *35*, 972–981. [[CrossRef](#)]
18. Rajak, D.K.; Pagar, D.D.; Menezes, P.L.; Eyvazian, A. Friction-based welding processes: Friction welding and friction stir welding. *J. Adhes. Sci. Technol.* **2020**, *34*, 2613–2637. [[CrossRef](#)]
19. Wang, H.; Gurevich, E.L.; Ostendorf, A. Femtosecond laser shock peening on the surface of NiTi shape memory alloy. *Procedia CIRP* **2021**, *94*, 910–913. [[CrossRef](#)]
20. Saleh, A. High-speed friction welding analysis. *J. Mech. Sci.* **2022**, *120*, 100564. [[CrossRef](#)]
21. Anggono, A.D.; Kholis, N.; Ngafwan, N. Structure and Mechanical Properties of Double Side Friction Stir Welded Aluminium AA6061 with the Addition of Cu Powder. *Mater. Sci. Forum* **2022**, *1051*, 111–118. [[CrossRef](#)]
22. Liu, Y.; Zhao, Z.; Zhang, C.; Wang, Q.; Sun, H.; Li, N. Corrigendum to ‘Characterization of the microstructure and the texture of inertia friction welding in TC25G titanium alloy [Mater. Lett. 277 (2020) 128329]. *Mater. Lett.* **2021**, *300*, 130052. [[CrossRef](#)]
23. El-Fahhar, H.H.; Gadallah, E.A.; Habba, M.I.; Seleman, M.M.E.S.; Ahmed, M.M.; Mohamed, A.Y.; Fouad, R.A. Effect of post-weld heat-treatment and solid-state thermomechanical treatment on the properties of the AA6082 MIG welded joints. *Sci. Rep.* **2024**, *14*, 4380. [[CrossRef](#)] [[PubMed](#)]
24. Li, Y.; Sun, Y.; Bai, X. Numerical simulation of the flow, solidification, and solute transport in a billet mold under electromagnetic stirring. *Met. Res. Technol.* **2021**, *118*, 221. [[CrossRef](#)]
25. Meyghani, B.; Awang, M.B.; Wu, C.S. Thermal analysis of friction stir welding with a complex curved welding seam. *Int. J. Eng.* **2019**, *32*, 1480–1484. [[CrossRef](#)]
26. Gkatzogiannis, S.; Weinert, J.; Engelhardt, I.; Knoedel, P.; Ummenhofer, T. Corrosion fatigue behaviour of HFMI-treated butt welds. *Int. J. Fatigue* **2021**, *145*, 106079. [[CrossRef](#)]
27. Zhao, Z.; Li, K.; Li, W.; Zhang, L. Cyclic ablation behavior of C/C-ZrC-SiC-ZrB₂ composites under oxyacetylene torch with two heat fluxes at the temperatures above 2000 °C. *Corros. Sci.* **2022**, *181*, 109202. [[CrossRef](#)]
28. Wang, W.; Han, P.; Peng, P.; Zhang, T.; Liu, Q.; Yuan, S.-N.; Huang, L.-Y.; Yu, H.-L.; Qiao, K.; Wang, K.-S. Friction Stir Processing of Magnesium Alloys: A Review. *Acta Met. Sin. Engl. Lett.* **2020**, *33*, 43–57. [[CrossRef](#)]
29. Yu, P.; Wu, C.; Shi, L. Analysis and characterization of dynamic recrystallization and grain structure evolution in friction stir welding of aluminum plates. *Acta Mater.* **2021**, *207*, 116692. [[CrossRef](#)]

Disclaimer/Publisher’s Note: The statements, opinions and data contained in all publications are solely those of the individual author(s) and contributor(s) and not of MDPI and/or the editor(s). MDPI and/or the editor(s) disclaim responsibility for any injury to people or property resulting from any ideas, methods, instructions or products referred to in the content.